

# World Journal of *Radiology*

*World J Radiol* 2022 June 28; 14(6): 114-179



**REVIEW**

- 114 Tuberculosis conundrum - current and future scenarios: A proposed comprehensive approach combining laboratory, imaging, and computing advances  
*Merchant SA, Shaikh MJS, Nadkarni P*

**MINIREVIEWS**

- 137 Recent advances in imaging techniques of renal masses  
*Aggarwal A, Das CJ, Sharma S*
- 151 Artificial intelligence technologies in nuclear medicine  
*Tamam MO, Tamam MC*

**ORIGINAL ARTICLE****Prospective Study**

- 155 Evaluation of the dual vascular supply patterns in ground-glass nodules with a dynamic volume computed tomography  
*Wang C, Wu N, Zhang Z, Zhang LX, Yuan XD*
- 165 Do preoperative pancreatic computed tomography attenuation index and enhancement ratio predict pancreatic fistula after pancreaticoduodenectomy?  
*Gnanasekaran S, Durgesh S, Gurram R, Kalayarasan R, Pottakkat B, Rajeswari M, Srinivas BH, Ramesh A, Sahoo J*

**LETTER TO THE EDITOR**

- 177 Comments on "Neonatal infratentorial subdural hematoma contributing to obstructive hydrocephalus in the setting of therapeutic cooling: A case report"  
*Siasios I, Fotiadou A, Rud Y*

**ABOUT COVER**

Editorial Board Member of *World Journal of Radiology*, Jaber S Alqahtani, MSc, PhD, Academic Research, Assistant Professor, Research Scientist, Department of Respiratory Care, Prince Sultan Military College of Health Sciences, Dammam 34313, Saudi Arabia. Alqahtani-Jaber@hotmail.com

**AIMS AND SCOPE**

The primary aim of *World Journal of Radiology (WJR, World J Radiol)* is to provide scholars and readers from various fields of radiology with a platform to publish high-quality basic and clinical research articles and communicate their research findings online.

*WJR* mainly publishes articles reporting research results and findings obtained in the field of radiology and covering a wide range of topics including state of the art information on cardiopulmonary imaging, gastrointestinal imaging, genitourinary imaging, musculoskeletal imaging, neuroradiology/head and neck imaging, nuclear medicine and molecular imaging, pediatric imaging, vascular and interventional radiology, and women's imaging.

**INDEXING/ABSTRACTING**

The *WJR* is now abstracted and indexed in Emerging Sources Citation Index (Web of Science), PubMed, PubMed Central, Reference Citation Analysis, China National Knowledge Infrastructure, China Science and Technology Journal Database, and Superstar Journals Database. The 2021 edition of Journal Citation Reports® cites the 2020 Journal Citation Indicator (JCI) for *WJR* as 0.51.

**RESPONSIBLE EDITORS FOR THIS ISSUE**

Production Editor: *Wen-Wen Qi*, Production Department Director: *Xu Guo*; Editorial Office Director: *Jia-Ping Yan*.

**NAME OF JOURNAL**

*World Journal of Radiology*

**ISSN**

ISSN 1949-8470 (online)

**LAUNCH DATE**

January 31, 2009

**FREQUENCY**

Monthly

**EDITORS-IN-CHIEF**

Thomas J Vogl

**EDITORIAL BOARD MEMBERS**

<https://www.wjgnet.com/1949-8470/editorialboard.htm>

**PUBLICATION DATE**

June 28, 2022

**COPYRIGHT**

© 2022 Baishideng Publishing Group Inc

**INSTRUCTIONS TO AUTHORS**

<https://www.wjgnet.com/bpg/gerinfo/204>

**GUIDELINES FOR ETHICS DOCUMENTS**

<https://www.wjgnet.com/bpg/GerInfo/287>

**GUIDELINES FOR NON-NATIVE SPEAKERS OF ENGLISH**

<https://www.wjgnet.com/bpg/gerinfo/240>

**PUBLICATION ETHICS**

<https://www.wjgnet.com/bpg/GerInfo/288>

**PUBLICATION MISCONDUCT**

<https://www.wjgnet.com/bpg/gerinfo/208>

**ARTICLE PROCESSING CHARGE**

<https://www.wjgnet.com/bpg/gerinfo/242>

**STEPS FOR SUBMITTING MANUSCRIPTS**

<https://www.wjgnet.com/bpg/GerInfo/239>

**ONLINE SUBMISSION**

<https://www.f6publishing.com>

## Prospective Study

## Evaluation of the dual vascular supply patterns in ground-glass nodules with a dynamic volume computed tomography

Chao Wang, Ning Wu, Zhuang Zhang, Lai-Xing Zhang, Xiao-Dong Yuan

**Specialty type:** Radiology, nuclear medicine and medical imaging**Provenance and peer review:** Unsolicited article; Externally peer reviewed.**Peer-review model:** Single blind**Peer-review report's scientific quality classification**Grade A (Excellent): 0  
Grade B (Very good): B  
Grade C (Good): C  
Grade D (Fair): D  
Grade E (Poor): 0**P-Reviewer:** Esch M, Germany;  
Konovalov AB, Russia**Received:** December 2, 2021**Peer-review started:** December 2, 2021**First decision:** April 8, 2022**Revised:** April 20, 2022**Accepted:** June 16, 2022**Article in press:** June 16, 2022**Published online:** June 28, 2022**Chao Wang, Zhuang Zhang, Lai-Xing Zhang,** Department of Graduate, Hebei North University, Zhangjiakou 075000, Hebei Province, China**Ning Wu, Xiao-Dong Yuan,** Department of Radiology, The Eighth Medical Center of the People's Liberation Army General Hospital, Beijing 100091, China**Corresponding author:** Xiao-Dong Yuan, MD, PhD, Chief Doctor, Professor, Department of Radiology, The Eighth Medical Center of the People's Liberation Army General Hospital, No. 17 Heishanhu Road, Haidian District, Beijing 100091, China. [yuanxiaodongzj@163.com](mailto:yuanxiaodongzj@163.com)**Abstract****BACKGROUND**

In recent years, the detection rate of ground-glass nodules (GGNs) has been improved dramatically due to the popularization of low-dose computed tomography (CT) screening with high-resolution CT technique. This presents challenges for the characterization and management of the GGNs, which depends on a thorough investigation and sufficient diagnostic knowledge of the GGNs. In most diagnostic studies of the GGNs, morphological manifestations are used to differentiate benignancy and malignancy. In contrast, few studies are dedicated to the assessment of the hemodynamics, *i.e.*, perfusion parameters of the GGNs.

**AIM**

To assess the dual vascular supply patterns of GGNs on different histopathology and opacities.

**METHODS**

Forty-seven GGNs from 47 patients were prospectively included and underwent the dynamic volume CT. Histopathologic diagnoses were obtained within two weeks after the CT examination. Blood flow from the bronchial artery [bronchial flow (BF)] and pulmonary artery [pulmonary flow (PF)] as well as the perfusion index (PI) = [PF/(PF + BF)] were obtained using first-pass dual-input CT perfusion analysis and compared respectively between different histopathology and lesion types (pure or mixed GGNs) and correlated with the attenuation values of the lesions using one-way ANOVA, student's *t* test and Pearson correlation analysis.

**RESULTS**

Of the 47 GGNs (mean diameter, 8.17 mm; range, 5.3-12.7 mm), 30 (64%) were

carcinoma, 6 (13%) were atypical adenomatous hyperplasia and 11 (23%) were organizing pneumonia. All perfusion parameters (BF, PF and PI) demonstrated no significant difference among the three conditions (all  $P > 0.05$ ). The PFs were higher than the BFs in all the three conditions (all  $P < 0.001$ ). Of the 30 GGN carcinomas, 14 showed mixed GGNs and 16 pure GGNs with a higher PI in the latter ( $P < 0.01$ ). Of the 17 benign GGNs, 4 showed mixed GGNs and 13 pure GGNs with no significant difference of the PI between the GGN types ( $P = 0.21$ ). A negative correlation ( $r = -0.76$ ,  $P < 0.001$ ) was demonstrated between the CT attenuation values and the PIs in the 30 GGN carcinomas.

### CONCLUSION

The GGNs are perfused dominantly by the PF regardless of its histopathology while the weight of the BF in the GGN carcinomas increases gradually during the progress of its opacification.

**Key Words:** Ground-glass nodules; Tomography; X-ray computed; Lung cancer; Perfusion computed tomography; Dual blood supply

©The Author(s) 2022. Published by Baishideng Publishing Group Inc. All rights reserved.

**Core Tip:** In this study, bronchial flow (BF) and pulmonary flow (PF) as well as perfusion index (PI) were obtained by using first-pass dual-input computed tomography perfusion analysis and compared respectively among different histopathological types and between pure and mixed ground-glass nodules (GGNs), then correlated with the attenuation values in forty-seven GGNs from 47 patients. We found that the GGNs are perfused dominantly by the PF regardless of histopathological types while the weight of the BF in the GGN carcinomas increases gradually during its opacification. Therefore, the PI may be a potentially useful biomarker for distinguishing indolent nodules from aggressive ones.

**Citation:** Wang C, Wu N, Zhang Z, Zhang LX, Yuan XD. Evaluation of the dual vascular supply patterns in ground-glass nodules with a dynamic volume computed tomography. *World J Radiol* 2022; 14(6): 155-164

**URL:** <https://www.wjgnet.com/1949-8470/full/v14/i6/155.htm>

**DOI:** <https://dx.doi.org/10.4329/wjr.v14.i6.155>

## INTRODUCTION

In recent years, more and more ground-glass nodules (GGNs) have been detected due to the application of low-dose screening with high-resolution computed tomography (CT)[1]. The rapidly increasing GGN cases requires appropriate management which depends on a thorough investigation and sufficient knowledge of the GGNs. In most diagnostic studies of the GGNs, morphological factors or nodular characteristics are used to differentiate benignancy and malignancy[2-6]. On the other hand, studies of the solid lesions suggested that the information of CT perfusion is helpful in identification and treatment planning[7-13]. A few studies have quantitatively measured iodine concentration to assess the blood supply status of the GGNs with promising outcomes[14]. Furthermore, quantification of the dual blood supply from the pulmonary and bronchial artery, *i.e.*, the pulmonary flow (PF) and bronchial flow (BF) in lung disorders is recently achieved with the first-pass dual-input perfusion analysis at a dynamic volume CT, producing helpful information for differentiations and treatment planning[15]. Therefore, this prospective study was designed to determine the patterns of the dual vascular supply in the GGNs on different histopathology and attenuation values (HU).

## MATERIALS AND METHODS

### Study population

The prospective study was approved by the Institution Ethics Committee. Written informed consent was obtained from all patients. Between Jan 2014 and May 2018, 50 patients who had been previously evaluated by non-contrast CT and had GGNs with an axial diameter  $> 5$  mm were prospectively enrolled into this study. All patients received histopathological diagnoses which were acquired by CT-guided puncture biopsy or surgical resection within 2 wk after the CT perfusion. Exclusion criteria were as follows: severe motion artifacts on the perfusion images that made it difficult to perform the perfusion analysis; patients receiving any antitumor treatment prior to the CT perfusion and contraindications to the administration of the iodinated contrast media. 1 patient with beam hardening artifacts

caused by the contrast agent in an ipsilateral subclavian vein and 2 patients who received antitumor treatment before the CT perfusion were excluded. Eventually, forty-seven patients (27 men and 20 women; mean age, 53 years; range, 35-69 years) with 47 GGNs were included in the statistical analysis.

The radiation dose of the dynamic CT was calculated from the dose-length product (DLP) listed in the exposure summary sheet generated by the CT equipment and multiplied by a k-factor of 0.014[16].

### **CT perfusion imaging technique**

Before the CT examination, all patients performed breath training by holding their breath during the dynamic CT scan procedure and otherwise adopted regularly shallow breathing.

First, unenhanced helical CT of the entire thorax was performed to determine the location of the GGN. Then, the dynamic volume CT perfusion was performed at a 320-row multidetector CT (Aquilion ONE, Toshiba Medical Systems, Otawara, Japan). With a dual-head power injector, 50 mL of non-ionic contrast medium with an iodine concentration of 370 mgI/mL (Iopromide, Bayer Schering, Berlin, Germany) was injected at a flow rate of 5 mL/s, followed by 20 mL of saline solution at the same rate. Five seconds after the start of the bolus injection, 15 intermittent low-dose volume acquisitions were made with 2 s intervals with no table movement.

The dynamic contrast-enhanced volume CT protocol was performed with the following parameters: 80 kV tube voltage, 80 mA tube current, 0.5 s gantry rotation speed and 0.5 mm slice thickness. The 16 cm coverage included both the lung hilum and the GGN. The first two volumes were acquired before the contrast medium arrived in the pulmonary artery (PA) and served as the baseline. The duration of the breath hold was approximately 30 s. The raw data were reconstructed with adaptive iterative dose reduction and automatically produced 0.5 mm slice thickness and 0.5 mm spacing images, resulting in 320 images per volume and a total of 4800 images for the entire perfusion dataset.

### **Data post-processing and analysis**

Post-processing was performed using perfusion software available on the CT equipment (Body Perfusion, dual-input maximum slope analysis, Toshiba Medical Systems, Otawara, Japan). The first step is volume registration. The registration is performed to correct for motion between the dynamic volumes and creates a registered volume series. The registered volumes were then loaded into the body perfusion analysis software.

Rectangular region of interests (ROIs) (mean area 1.0 cm<sup>2</sup>) was manually placed in the pulmonary artery trunk and the aorta at the level of the hilum to generate the TDCs representing the PA input function and the bronchial artery input function, respectively. An elliptical ROI was placed in the left atrium and the peak time of the left atrium tunneled dialysis catheters (TDCs) was used to differentiate pulmonary circulation (before the peak time point) and bronchial circulation (after the peak time point) [15]. A freehand ROI was drawn to encompass the lesion to generate the TDC of the contrast medium's first-pass attenuation in the GGN. The perfusion analysis range was set from -700 HU to 50 HU to confine the perfusion analysis to the GGN or mixed GGN regions only and to ignore normal lung parenchyma. Finally, 512 × 512 matrix color-coded maps of the PF, BF and perfusion index [PI = PF/(PF + BF)] were generated automatically. For each lesion, measurements were repeated on all relevant 5.0-mm axial slices and then averaged to calculate the final value. Lesion opacity (mean HU) was measured on the non-contrast axial slice with the maximum lesion diameter using a freehand ROI closely encompassing the lesion and avoiding major vessels. This post-processing procedure was independently performed by two radiologists (\*\*BLINDED\*\*, with 13 and 11 years of experience, respectively in CT perfusion in the abdomen and chest). Each radiologist was blinded to the results of the other and the histopathological diagnoses. The final results were the average of the two observers. Inter-observer reproducibility was assessed for the PF, BF and PI as well as the lesion opacity (mean HU). The lesion type (pure GGN or mixed GGN) was independently determined by the two radiologists and by a third radiologist (\*\*BLINDED\*\*) if the results of the two radiologists were inconsistent.

The pure GGN was defined as a focal, slightly increased attenuation in lung without masking the underlying structures on the lung window images while the mixed GGN as a focal increased attenuation with solid components masking the underlying structures of pulmonary vessels[17].

### **Statistical analysis**

Forty-seven GGNs were analyzed. The bronchial artery (BF) and pulmonary artery (PF) as well as the PI [= PF/(PF+BF)] were compared respectively between the histopathologic types and the lesion types (pure GGNs or mixed GGNs) using one-way ANOVA and students' *t* test and correlated respectively with lesions' HU using Pearson correlation analysis. In addition, the BF and PF were compared by paired *t* test to determine the dominant blood flow in the GGNs. The inter-observer reproducibility of perfusion parameters (BF, PF and PI) and HU of GGNs were assessed using intraclass correlation coefficients (ICC). Statistical analysis was performed using commercially available software (SPSS, V13.0, IBM). A *P* value < 0.05 was considered to indicate a significant difference.

## RESULTS

All patients showed good compliance with the CT perfusion procedure. No severe motion artifacts or adverse events occurred.

Of the 47 GGNs (mean diameter, 8.17 mm; range, 5.3-12.7 mm), 30 (64%) proved to be bronchioloalveolar cell carcinoma (BAC) ( $n = 24$ ) or adenocarcinoma with predominant BAC component ( $n = 6$ ), six (13%) atypical adenomatous hyperplasia and 11 (23%) organizing pneumonia. None of the three perfusion parameters demonstrated significant difference among the three histopathological types (Table 1). Of the 30 carcinomas GGNs, 14 showed mixed GGNs and 16 pure GGNs, with a greater PI in the latter ( $P < 0.01$ ). Of the 17 benign GGNs, 4 showed mixed GGNs (including 1 atypical adenomatous hyperplasia and 3 organizing pneumonia) and 13 pure GGNs (including 5 atypical adenomatous hyperplasia and 8 organizing pneumonia) with no significant difference of the PI between the GGN types ( $P = 0.21$ ). Of the 30 cancerous GGNs, the lesions' HU demonstrated mild negative correlation with the PF ( $r = -0.558$ ,  $P = 0.001$ ) while mild positive correlation with the BF ( $r = 0.565$ ,  $P = 0.001$ ). The PI demonstrates moderate negative correlation with the HU ( $r = -0.76$ ,  $P < 0.001$ ). No correlation between the perfusion parameters and the HU was revealed in the other two diseases (all  $P > 0.05$ ).

Perfusion parameters were visualized by color maps and fused onto the original axial CT images. Representative perfusion color maps are shown in Figure 1 and Figure 2. Statistical results of the perfusion parameters derived from dual-input computed tomography perfusion are listed in Table 1 and shown in Figures 3-5. ICC (0.94, 95%CI: 0.93-0.95) demonstrated that the reproducibility between the two observers is good.

The dynamic volume CT perfusion protocol was identical for all 47 cases. The CT dose DLP = 324.8 mGy cm or 4.55 mSv ( $k = 0.014$ ).

## DISCUSSION

The PF and the BF, *i.e.*, the dual vascular supply was revealed in lung cancer through post-mortem microarteriography in the early 1970s[18]. Since then, the BF in lung cancer was confirmed by many reports and broncho angiography studies[19]. In contrast, PF in lung cancer was rarely reported until recently with an *in vivo* evaluation of the dual vascular supply in lung cancer and was achieved by using a dynamic contrast-enhanced volume CT[20] which reported a dominant BF along with a subordinate PF in solid cancerous nodules. In the present investigation, however, we revealed a dominant PF along with a subordinate BF in the GGN carcinomas. In addition, we revealed that with the increase of the lesion opacity, the weight of the PF in the total blood flow of the GGN carcinomas decreases while the weight of the BF increases. Thus, we would like to provide an interpretation of our findings combining with the findings of the previous reports as the following: During the progress of the lung adenocarcinoma from a pure GGN to a mixed GGN then to a solid nodule[21,22], the PF dominant perfusion pattern may gradually reverse to the BF dominant perfusion pattern. In contrast to solid nodular carcinoma, GGN carcinoma are supposed to be indolent, which allows long-term follow-up of their morphological changes for treatment planning[23-25]. Our findings on the increasing weight of the BF in GGNs during its opacification suggest that the PI which represents the weight of the BF in the total blood supply (BF + PF) may be a potentially useful biomarker for distinguishing indolent nodules from active ones.

Though the dual vascular supply patterns of the GGNs were determined in the current investigation, it cannot help differentiate GGNs between benignancy and malignancy because none of the three perfusion parameters (PF, BF and PI) showed significant difference between benign and malignant GGNs. Nevertheless, the feature of the PF dominant perfusion in the GGN carcinomas may have two important clinical implications: (1) Bronchial arterial chemoembolization may not be suitable for the treatment of a GGN carcinoma; and (2) radiation therapy may not be suitable for the treatment of a GGN carcinoma. The reason for the former is self-evident. The reason for the latter is because the PF dominant perfusion indicates a low level of oxygenation in the GGN carcinoma resulting in a low level of radiosensitivity[20,26].

It was reported that the pure GGNs are difficult to be distinguished morphologically between malignancy and benignancy[27]; however, the mixed GGNs tend to be a malignant one[28,29]. During a long-term CT follow-up of an adenocarcinoma in the lung, the typical case may be a pure GGN at the very beginning then gradually changing into a mixed GGN and a solid nodule at last[30,31]. Therefore, it strongly suggests an adenocarcinoma when a pure GGN gradually changed into a mixed one during follow-up. According to the current investigation, a pure GGN carcinoma is mainly perfused by the PF while the weight of the BF increases in a mixed GGN. In addition, a solid carcinoma is mainly perfused by the BF according to the previous study[15,20,32]. These adaptive changes of the perfusion patterns may bring more oxygen to feed the growth of the GGN carcinomas because of a low oxygen level in the PF and a high oxygen level in the BF. However, the mechanism behind these changes is still unknown and needs to be investigated further.

**Table 1 Results of histopathologic comparisons on the three perfusion parameters**

Parameters	Histopathology	n	mean ± SD	95% CI		One way ANOVA
				Lower	Upper	
PF (mL/min/100 mL)	Carcinoma	30	135.54 ± 46.58	118.15	152.93	<i>P</i> = 0.435
	Adenomatous hyperplasia	6	121.51 ± 40.56	78.94	164.08	
	Organizing pneumonia	11	116.06 ± 43.15	87.07	145.05	
BF (mL/min/100 mL)	Carcinoma	30	33.21 ± 12.12	28.68	37.74	<i>P</i> = 0.079
	Adenomatous hyperplasia	6	26.55 ± 4.08	22.26	30.83	
	Organizing pneumonia	11	24.96 ± 9.90	18.31	31.61	
PI (100%)	Carcinoma	30	0.79 ± 0.09	0.75	0.82	<i>P</i> = 0.657
	Adenomatous hyperplasia	6	0.80 ± 0.07	0.73	0.88	
	Organizing pneumonia	11	0.81 ± 0.69	0.76	0.86	

PF: Pulmonary flow; BF: Bronchial flow; PI: Perfusion index.

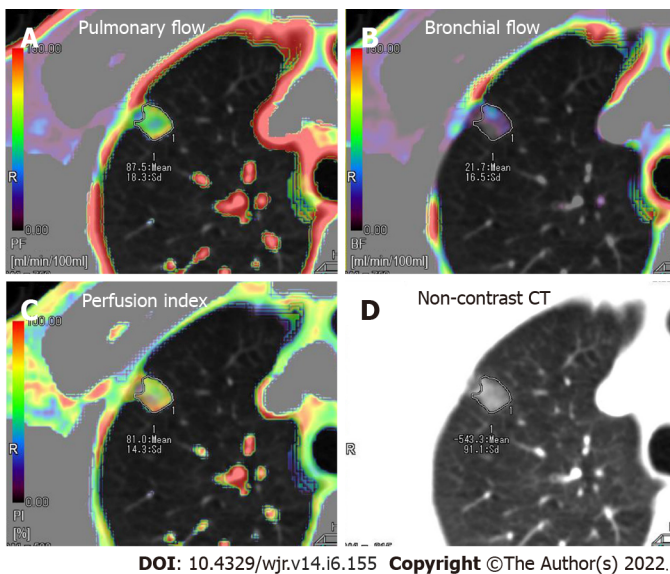
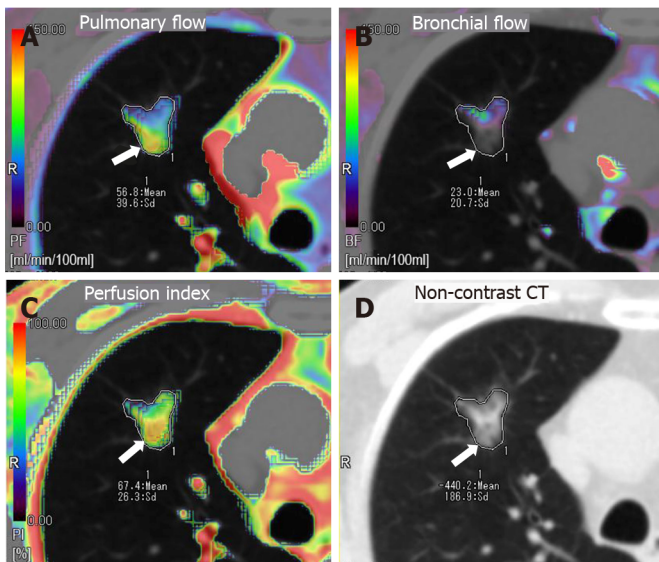


**Figure 1 Axial colored perfusion maps in a 55-year-old male patient with pure ground-glass nodule carcinoma located in the right superior lung.** Dominant pulmonary flow (PF) along with subordinate bronchial flow (BF) was observed in the pure ground-glass nodule. A: Axial colored perfusion map of PF; B: Axial colored perfusion map of BF; C: Axial colored perfusion map of perfusion index; D: Axial non-contrast computed tomography.

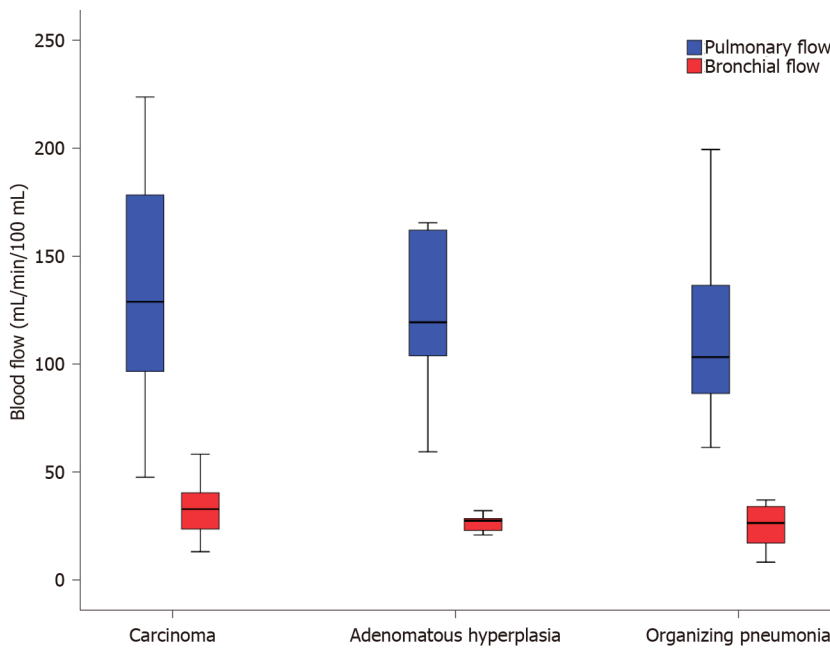
In this investigation, the perfusion analysis range was set from -700 HU to 50 HU to confine the perfusion analysis to the GGN or mixed GGN while ignore the normal lung parenchyma. In fact, the perfusion analysis range could be set individually according to an on-spot CT measurement of the GGN. To simplify and standardize the post-processing procedure, we adopted a fixed CT perfusion analysis range, *i.e.*, -700 HU to 50 HU in this study.

There are some limitations to this study. First, the relatively small sample size of this study will undermine the significance of our findings. Second, a relatively high radiation dose is an unavoidable limitation of perfusion CT though the total effective dose of each patient was controlled to comparable with a multiphase CT procedure[33,34]. Third, although the difference of CT perfusion between the pure and mixed GGN carcinomas was investigated, the solid components and the pure components of the mixed GGN carcinomas were not evaluated separately because it's difficult to define the boundary of the two components. Fourth, our findings cannot help to differentiate between malignant and benign GGNs because no significant difference in perfusion parameters was revealed between them. However, the change regularity of the dual vascular supply patterns during the opacification of GGN carcinomas could help to better understand its biological behavior and therefore help to better manage it.



DOI: 10.4329/wjr.v14.i6.155 Copyright ©The Author(s) 2022.

**Figure 2** Axial colored perfusion maps in a 72-year-old male patient with mixed ground-glass nodule carcinoma located in the right superior lung. The perfusion is heterogeneous throughout the lesion. Pulmonary flow (PF) is globally dominant, especially in the dorsal part of the lesion (arrow), which corresponds to the lower attenuation region of the mixed ground-glass nodule. A: Axial colored perfusion map of PF; B: Axial colored perfusion map of bronchial flow; C: Axial colored perfusion map of perfusion index; D: Axial non-contrast computed tomography.



DOI: 10.4329/wjr.v14.i6.155 Copyright ©The Author(s) 2022.

**Figure 3** Box plot of perfusion parameters demonstrates dominant Pulmonary flow (PF) along with relatively low bronchial flow (BF) in carcinoma ( $n = 30$ ), atypical adenomatous hyperplasia ( $n = 6$ ) and organizing pneumonia ( $n = 11$ ).

## CONCLUSION

In conclusion, the GGNs are perfused dominantly by the PF regardless of its histopathology while the weight of the BF in the GGN carcinomas increases gradually during its opacification. The PI may be a potentially useful biomarker for distinguishing indolent nodules from aggressive ones.

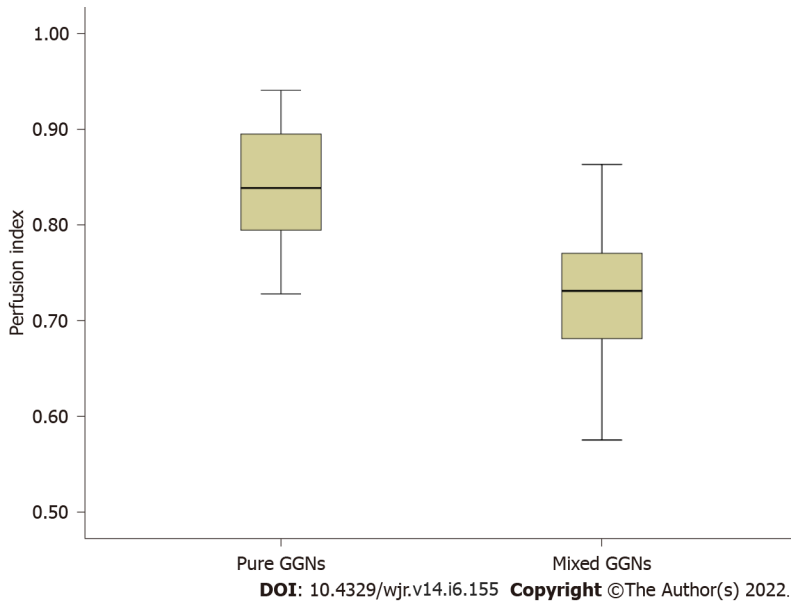


**Figure 4** Box plot of perfusion index [= pulmonary flow/(pulmonary flow + bronchial flow)] demonstrates dominant pulmonary flow along with subordinate bronchial flow in pure ground-glass nodule carcinoma ( $n = 16$ ) and a weakened pulmonary flow along with an enhanced bronchial flow in mixed ground-glass nodule carcinoma.

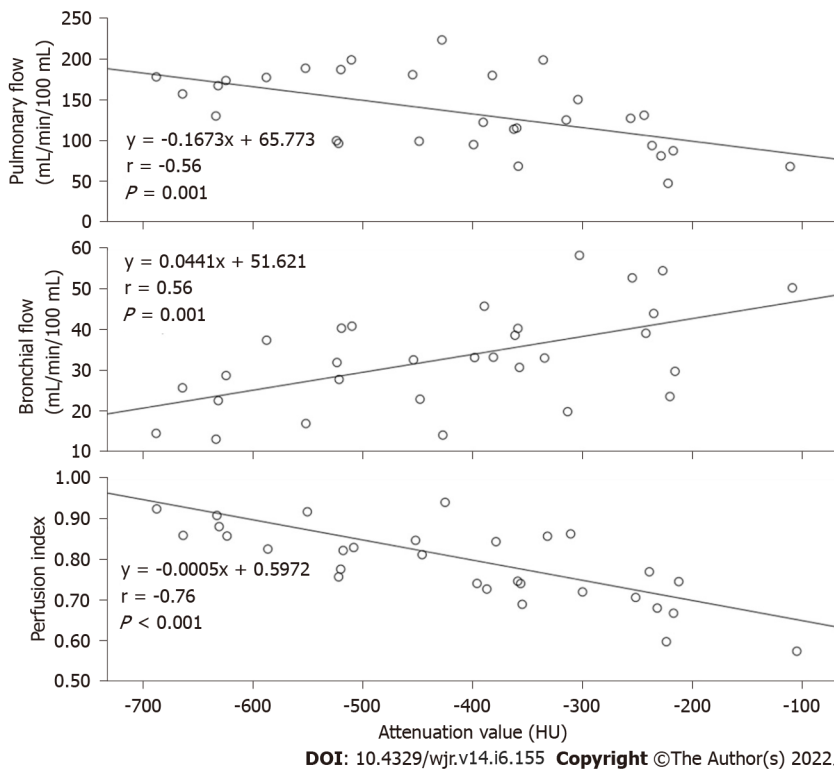


**Figure 5** Plots of the Pearson correlation between the attenuation values of the ground-glass nodule carcinoma and the three perfusion parameters. The HU of the GGN carcinoma correlates negatively, positively and negatively with the pulmonary flow (PF), bronchial flow (BF) and the perfusion index (PI), respectively. A: Correlation between the HU of ground-glass nodule (GGN) carcinoma and PF; B: Correlation between the HU of GGN carcinoma and BF; C: Correlation between the HU of GGN carcinoma and PI.

## ARTICLE HIGHLIGHTS

### Research background

In recent years, the detection rate of ground-glass nodules (GGNs) has been improved dramatically due to the application of low-dose computed tomography (CT) screening and high-resolution CT. The rapidly increasing detection rate requires appropriate managements of the GGNs which depends on a thorough investigation and sufficient knowledge of the GGNs. In most diagnostic studies of the GGNs, morphological factors are used to differentiate benignancy and malignancy. However, evaluation of the dual vascular supply patterns in GGNs with a dynamic volume CT could provide more valuable information for identification and treatment planning.

### Research motivation

Studies of the solid lesions suggested that the information of CT perfusion is helpful in identification and treatment planning. Furthermore, quantification of the dual blood supply from the pulmonary and bronchial artery, *i.e.*, the pulmonary flow (PF) and bronchial flow (BF) in lung disorders was recently achieved with a dynamic volume CT and the first-pass dual-input perfusion analysis producing helpful information for differentiations and treatment planning. Based on this, our study is devoted to the assessment of the dual blood supply pattern of GGNs by dynamic CT to provide more valuable information for differentiations and treatment planning.

### Research objectives

To assess the dual vascular supply patterns of GGNs with regard to different histopathology and opacities using a dynamic volume CT.

### Research methods

In this prospective study, 47 GGNs from 47 patients were included and underwent the dynamic volume CT. Histopathologic diagnoses were obtained within two weeks after the CT examination. BF and PF as well as the perfusion index [(PI) = PF / (PF+BF)] were obtained using first-pass dual-input CT perfusion analysis and compared respectively between different histopathology and lesion types (pure or mixed GGN) and correlated with the attenuation values of the lesions, using one-way ANOVA, student's *t* test and Pearson correlation analysis.

### Research results

Forty-seven GGNs including three histopathological types (30 carcinoma, 6 atypical adenomatous hyperplasia and 11 organizing pneumonia). All perfusion parameters (BF, PF and PI) demonstrated no significant difference among the three conditions (all  $P > 0.05$ ). The PFs were higher than the BFs in all the three conditions (all  $P < 0.001$ ). Of the 30 GGN carcinomas, 14 showed mixed GGNs and 16 pure GGNs, with a higher PI in the latter ( $P < 0.01$ ). A negative correlation ( $r = -0.76$ ,  $P < 0.001$ ) was demonstrated between the CT attenuation values and the PIs in the 30 GGN carcinomas.

### Research conclusions

In conclusion, the GGNs are perfused dominantly by the PF regardless of its histopathology while the weight of the BF in the GGN carcinomas increases gradually during the progress of its opacification.

### Research perspectives

Our future study will expand the GGNs sample size to further investigate potential difference of perfusion parameters between malignant and benign GGNs and to further confirm that the PI is a useful biomarker for distinguishing indolent GGNs carcinomas from aggressive ones.

## FOOTNOTES

**Author contributions:** Yuan XD and Wu N designed the study; Wang C wrote the first draft of the manuscript; Zhang Z and Zhang LX collected the data; Wang C performed the literature search and analysis; Yuan XD and Wang C conducted the statistical analysis and polished the language; all authors participated in and approved the final manuscript.

**Supported by** the National Natural Science Foundation of China, No. 81671680.

**Institutional review board statement:** Our prospective study was approved by our institutional review board.

**Informed consent statement:** Written informed consents were obtained from all patients.

**Conflict-of-interest statement:** The authors of this manuscript having no conflicts of interest to disclose.

**Data sharing statement:** No additional data are available.

**Open-Access:** This article is an open-access article that was selected by an in-house editor and fully peer-reviewed by external reviewers. It is distributed in accordance with the Creative Commons Attribution NonCommercial (CC BY-NC 4.0) license, which permits others to distribute, remix, adapt, build upon this work non-commercially, and license their derivative works on different terms, provided the original work is properly cited and the use is non-commercial. See: <https://creativecommons.org/licenses/by-nc/4.0/>

**Country/Territory of origin:** China

**ORCID number:** Chao Wang 0000-0003-3446-9045; Ning Wu 0000-0002-9307-3115; Zhuang Zhang 0000-0002-9270-8342; Lai-Xing Zhang 0000-0001-7034-8043; Xiao-Dong Yuan 0000-0003-1964-5098.

**S-Editor:** Zhang H

**L-Editor:** Filipodia CL

**P-Editor:** Zhang H

## REFERENCES

- 1 **Tsutsui S**, Ashizawa K, Minami K, Tagawa T, Nagayasu T, Hayashi T, Uetani M. Multiple focal pure ground-glass opacities on high-resolution CT images: Clinical significance in patients with lung cancer. *AJR Am J Roentgenol* 2010; **195**: W131-W138 [PMID: 20651172 DOI: 10.2214/AJR.09.3828]
- 2 **Lee HY**, Choi YL, Lee KS, Han J, Zo JI, Shim YM, Moon JW. Pure ground-glass opacity neoplastic lung nodules: histopathology, imaging, and management. *AJR Am J Roentgenol* 2014; **202**: W224-W233 [PMID: 24555618 DOI: 10.2214/AJR.13.11819]
- 3 **Yang J**, Wang H, Geng C, Dai Y, Ji J. Advances in intelligent diagnosis methods for pulmonary ground-glass opacity nodules. *Biomed Eng Online* 2018; **17**: 20 [PMID: 29415726 DOI: 10.1186/s12938-018-0435-2]
- 4 **Hu H**, Wang Q, Tang H, Xiong L, Lin Q. Multi-slice computed tomography characteristics of solitary pulmonary ground-glass nodules: Differences between malignant and benign. *Thorac Cancer* 2016; **7**: 80-87 [PMID: 26913083 DOI: 10.1111/1759-7714.12280]
- 5 **Jiang B**, Takashima S, Miyake C, Hakucho T, Takahashi Y, Morimoto D, Numasaki H, Nakanishi K, Tomita Y, Higashiyama M. Thin-section CT findings in peripheral lung cancer of 3 cm or smaller: are there any characteristic features for predicting tumor histology or do they depend only on tumor size? *Acta Radiol* 2014; **55**: 302-308 [PMID: 23926233 DOI: 10.1177/0284185113495834]
- 6 **Meng Y**, Liu CL, Cai Q, Shen YY, Chen SQ. Contrast analysis of the relationship between the HRCT sign and new pathologic classification in small ground glass nodule-like lung adenocarcinoma. *Radiol Med* 2019; **124**: 8-13 [PMID: 30191447 DOI: 10.1007/s11547-018-0936-x]
- 7 **Zhang M**, Kono M. Solitary pulmonary nodules: evaluation of blood flow patterns with dynamic CT. *Radiology* 1997; **205**: 471-478 [PMID: 9356631 DOI: 10.1148/radiology.205.2.9356631]
- 8 **Lee YH**, Kwon W, Kim MS, Kim YJ, Lee MS, Yong SJ, Jung SH, Chang SJ, Sung KJ. Lung perfusion CT: the differentiation of cavitory mass. *Eur J Radiol* 2010; **73**: 59-65 [PMID: 19481401 DOI: 10.1016/j.ejrad.2009.04.037]
- 9 **Boll DT**, Merkle EM. Differentiating a chronic hyperplastic mass from pancreatic cancer: a challenge remaining in multidetector CT of the pancreas. *Eur Radiol* 2003; **13** Suppl 5: M42-M49 [PMID: 14989611 DOI: 10.1007/s00330-003-2100-8]
- 10 **Coolen J**, Vansteenkiste J, De Keyzer F, Decaluwé H, De Wever W, Deroose C, Doods C, Verbeken E, De Leyn P, Vandecaveye V, Van Raemdonck D, Nackaerts K, Dymarkowski S, Verschakelen J. Characterisation of solitary pulmonary lesions combining visual perfusion and quantitative diffusion MR imaging. *Eur Radiol* 2014; **24**: 531-541 [PMID: 24173597 DOI: 10.1007/s00330-013-3053-1]
- 11 **Bellomi M**, Petralia G, Sonzogni A, Zampino MG, Rocca A. CT perfusion for the monitoring of neoadjuvant chemotherapy and radiation therapy in rectal carcinoma: initial experience. *Radiology* 2007; **244**: 486-493 [PMID: 17641369 DOI: 10.1148/radiol.2442061189]
- 12 **Li XS**, Fan HX, Fang H, Huang H, Song YL, Zhou CW. Value of whole-tumor dual-input perfusion CT in predicting the effect of multiarterial infusion chemotherapy on advanced non-small cell lung cancer. *AJR Am J Roentgenol* 2014; **203**: W497-W505 [PMID: 25341164 DOI: 10.2214/AJR.13.11621]
- 13 **Lin G**, Sui Y, Li Y, Huang W. Diagnostic and prognostic value of CT perfusion parameters in patients with advanced NSCLC after chemotherapy. *Am J Transl Res* 2021; **13**: 13516-13523 [PMID: 35035693]
- 14 **Liu G**, Li M, Li G, Li Z, Liu A, Pu R, Cao H, Liu Y. Assessing the Blood Supply Status of the Focal Ground-Glass Opacity in Lungs Using Spectral Computed Tomography. *Korean J Radiol* 2018; **19**: 130-138 [PMID: 29354009 DOI: 10.3348/kjr.2018.19.1.130]
- 15 **Yuan X**, Zhang J, Ao G, Quan C, Tian Y, Li H. Lung cancer perfusion: can we measure pulmonary and bronchial circulation simultaneously? *Eur Radiol* 2012; **22**: 1665-1671 [PMID: 22415414 DOI: 10.1007/s00330-012-2414-5]
- 16 **Valentin J**; International Commission on Radiation Protection. Managing patient dose in multi-detector computed tomography(MDCT). ICRP Publication 102. *Ann ICRP* 2007; **37**: 1-79, iii [PMID: 18069128 DOI: 10.1016/j.icrp.2007.09.001]
- 17 **Godoy MC**, Naidich DP. Overview and strategic management of subsolid pulmonary nodules. *J Thorac Imaging* 2012; **27**: 240-248 [PMID: 22847591 DOI: 10.1097/RTI.0b013e31825d515b]

- 18 **Milne EN.** Circulation of primary and metastatic pulmonary neoplasms. A postmortem microarteriographic study. *Am J Roentgenol Radium Ther Nucl Med* 1967; **100**: 603-619 [PMID: [5230250](#) DOI: [10.2214/ajr.100.3.603](#)]
- 19 **Luo L, Wang H, Ma H, Zou H, Li D, Zhou Y.** [Analysis of 41 cases of primary hypervascular non-small cell lung cancer treated with embolization of emulsion of chemotherapeutics and iodized oil]. *Zhongguo Fei Ai Za Zhi* 2010; **13**: 540-543 [PMID: [20677656](#) DOI: [10.3779/j.issn.1009-3419.2010.05.29](#)]
- 20 **Yuan X, Zhang J, Quan C, Cao J, Ao G, Tian Y, Li H.** Differentiation of malignant and benign pulmonary nodules with first-pass dual-input perfusion CT. *Eur Radiol* 2013; **23**: 2469-2474 [PMID: [23793548](#) DOI: [10.1007/s00330-013-2842-x](#)]
- 21 **Takashima S, Maruyama Y, Hasegawa M, Yamanda T, Honda T, Kadoya M, Sone S.** CT findings and progression of small peripheral lung neoplasms having a replacement growth pattern. *AJR Am J Roentgenol* 2003; **180**: 817-826 [PMID: [12591704](#) DOI: [10.2214/ajr.180.3.1800817](#)]
- 22 **Min JH, Lee HY, Lee KS, Han J, Park K, Ahn MJ, Lee SJ.** Stepwise evolution from a focal pure pulmonary ground-glass opacity nodule into an invasive lung adenocarcinoma: an observation for more than 10 years. *Lung Cancer* 2010; **69**: 123-126 [PMID: [20478641](#) DOI: [10.1016/j.lungcan.2010.04.022](#)]
- 23 **Mironova V, Blasberg JD.** Evaluation of ground glass nodules. *Curr Opin Pulm Med* 2018; **24**: 350-354 [PMID: [29634577](#) DOI: [10.1097/MCP.0000000000000492](#)]
- 24 **Pedersen JH, Saghir Z, Wille MM, Thomsen LH, Skov BG, Ashraf H.** Ground-Glass Opacity Lung Nodules in the Era of Lung Cancer CT Screening: Radiology, Pathology, and Clinical Management. *Oncology (Williston Park)* 2016; **30**: 266-274 [PMID: [26984222](#)]
- 25 **Lee GD, Park CH, Park HS, Byun MK, Lee IJ, Kim TH, Lee S.** Lung Adenocarcinoma Invasiveness Risk in Pure Ground-Glass Opacity Lung Nodules Smaller than 2 cm. *Thorac Cardiovasc Surg* 2019; **67**: 321-328 [PMID: [29359309](#) DOI: [10.1055/s-0037-1612615](#)]
- 26 **Ohno Y, Fujisawa Y, Koyama H, Kishida Y, Seki S, Sugihara N, Yoshikawa T.** Dynamic contrast-enhanced perfusion area-detector CT assessed with various mathematical models: Its capability for therapeutic outcome prediction for non-small cell lung cancer patients with chemoradiotherapy as compared with that of FDG-PET/CT. *Eur J Radiol* 2017; **86**: 83-91 [PMID: [28027771](#) DOI: [10.1016/j.ejrad.2016.11.008](#)]
- 27 **Kim HY, Shim YM, Lee KS, Han J, Yi CA, Kim YK.** Persistent pulmonary nodular ground-glass opacity at thin-section CT: histopathologic comparisons. *Radiology* 2007; **245**: 267-275 [PMID: [17885195](#) DOI: [10.1148/radiol.2451061682](#)]
- 28 **Bach PB, Silvestri GA, Hanger M, Jett JR; American College of Chest Physicians.** Screening for lung cancer: ACCP evidence-based clinical practice guidelines (2nd edition). *Chest* 2007; **132**: 69S-77S [PMID: [17873161](#) DOI: [10.1378/chest.07-1349](#)]
- 29 **Cha MJ, Lee KS, Kim HS, Lee SW, Jeong CJ, Kim EY, Lee HY.** Improvement in imaging diagnosis technique and modalities for solitary pulmonary nodules: from ground-glass opacity nodules to part-solid and solid nodules. *Expert Rev Respir Med* 2016; **10**: 261-278 [PMID: [26751340](#) DOI: [10.1586/17476348.2016.1141053](#)]
- 30 **Sawada S, Yamashita N, Sugimoto R, Ueno T, Yamashita M.** Long-term Outcomes of Patients With Ground-Glass Opacities Detected Using CT Scanning. *Chest* 2017; **151**: 308-315 [PMID: [27435815](#) DOI: [10.1016/j.chest.2016.07.007](#)]
- 31 **Bueno J, Landeras L, Chung JH.** Updated Fleischner Society Guidelines for Managing Incidental Pulmonary Nodules: Common Questions and Challenging Scenarios. *Radiographics* 2018; **38**: 1337-1350 [PMID: [30207935](#) DOI: [10.1148/rg.2018180017](#)]
- 32 **Nguyen-Kim TD, Frauenfelder T, Strobel K, Veit-Haibach P, Huellner MW.** Assessment of bronchial and pulmonary blood supply in non-small cell lung cancer subtypes using computed tomography perfusion. *Invest Radiol* 2015; **50**: 179-186 [PMID: [25500892](#) DOI: [10.1097/RLI.0000000000000124](#)]
- 33 **Tsai HY, Tung CJ, Yu CC, Tyan YS.** Survey of computed tomography scanners in Taiwan: dose descriptors, dose guidance levels, and effective doses. *Med Phys* 2007; **34**: 1234-1243 [PMID: [17500455](#) DOI: [10.1118/1.2712412](#)]
- 34 **Galanski M, Nagel HD, Stamm G.** [Results of a federation inquiry 2005/2006: pediatric CT X-ray practice in Germany]. *Rofö* 2007; **179**: 1110-1111 [PMID: [17955412](#) DOI: [10.1055/s-2007-992844](#)]



Published by **Baishideng Publishing Group Inc**  
7041 Koll Center Parkway, Suite 160, Pleasanton, CA 94566, USA  
**Telephone:** +1-925-3991568  
**E-mail:** [bpgoffice@wjgnet.com](mailto:bpgoffice@wjgnet.com)  
**Help Desk:** <https://www.f6publishing.com/helpdesk>  
<https://www.wjgnet.com>

